

AMP-ACTIVATED PROTEIN KINASE ACTIVATION IMPACTS ACINAR  
CELL PROLIFERATION AND SALIVARY FLOW RATES FOLLOWING  
RADIATION THERAPY

by

Rachel K. Meyer

---

Copyright © Rachel K. Meyer 2019

A Thesis Submitted to the Faculty of the  
DEPARTMENT OF NUTRITIONAL SCIENCES

In Partial Fulfillment of the Requirements

For the Degree of

MASTER OF SCIENCE

In the Graduate College

UNIVERSITY OF ARIZONA

2019

THE UNIVERSITY OF ARIZONA  
GRADUATE COLLEGE

As members of the Master's Committee, we certify that we have read the thesis prepared by **Rachel K. Meyer** titled **AMP-ACTIVATED PROTEIN KINASE ACTIVATION IMPACTS ACINAR CELL PROLIFERATION AND SALIVARY FLOW RATES FOLLOWING RADIATION THERAPY** and recommend that it be accepted as fulfilling the thesis requirement for the Master's Degree.



*Dr. Kirsten Limesand*

Date: 6/7/2019



*Dr. Frank Duca*

Date: 6/7/2019



*Dr. Jessica A. Martinez*

Date: 6/7/2019

Final approval and acceptance of this thesis is contingent upon the candidate's submission of the final copies of the thesis to the Graduate College.



I hereby certify that I have read this thesis prepared under my direction and recommend that it be accepted as fulfilling the Master's requirement.



*Dr. Kirsten Limesand*

Date: 6/7/2019

*Department of Nutritional Sciences*

A large, light blue, stylized watermark of the word 'ARIZONA' is positioned in the background of the lower half of the page.

## Table of Contents

<b>List of figures</b> .....	<b>4</b>
<b>Abstract</b> .....	<b>5</b>
<b>Introduction</b> .....	<b>6</b>
<i>Background</i> .....	8
<i>Objectives and Hypotheses</i> .....	10
<b>Materials and Methods</b> .....	<b>11</b>
<i>Ethics Statement</i> .....	11
<i>Mice</i> .....	11
<i>Radiation</i> .....	11
<i>Western Blot</i> .....	12
<i>qRT-PCR</i> .....	12
<i>Immunofluorescence Staining and Imaging</i> .....	12
<i>Saliva collection</i> .....	13
<i>Statistical Analysis</i> .....	13
<b>Results</b> .....	<b>14</b>
<i>NAD<sup>+</sup> and AMP levels are lower in parotid salivary gland tissue five days following radiation</i> .....	14
<i>Radiation suppresses parotid salivary gland AMPK phosphorylation and expression of NAMPT and SIRT1</i> .....	14
<i>AICAR treatment decreases compensatory proliferation of parotid acinar cells at D6 and D7 following radiation</i> .....	15
<i>AMPK activation with either AICAR or Metformin improves salivary output 30 days following radiation</i> .....	15
<b>Discussion</b> .....	<b>16</b>
<i>AMPK Activation, Proliferation and Salivary Output</i> .....	16
<i>Metformin and Untreated Mice</i> .....	16
<i>Alteration in the AMPK/SIRT1 Axis Following IR</i> .....	17
<i>Future Directions and Conclusion</i> .....	18
<b>References</b> .....	<b>24</b>

**List of Figures.**

*Figure 1. NAD<sup>+</sup> and AMP levels are lower in parotid salivary gland tissue five days following radiation.*.....20

*Figure 2. Radiation suppresses parotid salivary gland AMPK phosphorylation and expression of NAMPT and SIRT1.*.....21

*Figure 3. AICAR treatment decreases compensatory proliferation of parotid acinar cells at D6 and D7 following radiation.*.....22

*Figure 4. AMPK activation with either AICAR or Metformin improves salivary output 30 days following radiation.* .....23

*Figure 5. Schematic representation of the role of AMP-activated protein kinase (AMPK) in radiation-induced damage to salivary glands.* . . . . .24

## **Abstract**

Head and neck cancers remain the sixth most common cancer worldwide and represent over 600,000 new cases diagnosed annually. Typical treatment of early-stage head and neck cancers includes either surgery or radiotherapy; however, advanced cases often require surgery followed by radiation and chemotherapy. Salivary gland damage following radiotherapy leads to severe and chronic hypofunction with decreased salivary output, xerostomia, impaired ability to chew and swallow, a greatly increased risk of developing oral mucositis, and malnutrition. There is currently no standard of care for radiation induced salivary gland dysfunction; treatment is often limited to palliative treatment that provides only temporary relief. AMP-activated protein kinase (AMPK) is an enzyme that activates catabolic processes and has been shown to influence the cell cycle, proliferation, and autophagy. Additionally, AMPK has been implicated in the cellular response to radiation. In the present study, we found that radiation (IR) decreased tissue levels of phosphorylated AMPK, as well as NAD<sup>+</sup> and AMP. Further, expression of Sirtuin-1 and nicotinamide phosphoribosyl transferase (NAMPT) was lower five days following IR. Treatment with AMPK activator AICAR attenuated compensatory proliferation following IR, and both AICAR and Metformin treatment reversed chronic salivary gland dysfunction post-IR. Taken together, these data suggest that AMPK may be a novel therapeutic target for treatment of radiation-induced salivary damage.

## Introduction

Head and neck cancers remain the sixth most common cancer worldwide and represent over 600,000 new cases diagnosed annually.<sup>1</sup> Of these cases, over 90% are squamous cell carcinomas of the mucosal layer of the oral cavity, oropharynx, and larynx, and are most commonly associated with tobacco and alcohol use.<sup>1</sup> Worldwide incidence of these cancers varies considerably due to declining tobacco use in developed countries compared to widespread use in South and Southeast Asia.<sup>1,2</sup> In these countries, head and neck squamous cell carcinoma is the most common cancer in men and the third most common in women, accounting for an estimated 25% of all new cancer diagnoses.<sup>2</sup> As it stands, France has the highest incidence of this type of cancer among European countries, representing 5.5% of all cancers.<sup>2</sup> Other regions heavily affected by head and neck squamous cell carcinoma include Brazil and other areas of South America, Pacific islands including Papua New Guinea, and countries in Eastern Europe including Hungary, Slovakia, and Slovenia.<sup>2</sup>

Despite declining rates of tobacco use in areas of high socioeconomic status, cases of oropharyngeal squamous cell carcinoma (OSSC) are rising in these regions, with cases of OSSC increasing in the US by over 200% from 1988-2004.<sup>3</sup> This has been attributed to human papilloma virus-associated tumors.<sup>3</sup> Recently, a link between human papilloma virus (HPV) infection and oropharyngeal squamous cell carcinoma incidence has been identified via epidemiological studies that show a concurrent increase in OSCC incidence and HPV-positive tumors.<sup>4</sup> This association is of major concern due to the high prevalence of HPV worldwide; it is suggested that almost all sexually active adults will be exposed to some form of HPV in their lifetime.<sup>5</sup> Further, patients with HPV-positive OSCC tend to be younger and do not use tobacco or alcohol,<sup>4,6</sup> indicating a greater need for advances in care to reduce comorbidities and improve quality of life for patients following radiation and chemotherapy for head and neck cancers.

Although incidence of head and neck cancers are rising in parts of the world, treatment options remain limited.<sup>6</sup> Typical treatment of early-stage head and neck cancers includes either surgery or radiotherapy; however, advanced cases often require surgery followed by radiation and chemotherapy.<sup>3</sup> Although treatment options and survival rates vary heavily depending on the location and severity of malignancy, thousands of cancer survivors retain impaired quality of life following treatment due to secondary damage to surrounding tissues, including the salivary glands.<sup>7</sup>

Salivary gland damage following radiotherapy leads to severe and chronic hypofunction with decreased salivary output, xerostomia, impaired ability to chew and swallow, a greatly increased risk of developing oral mucositis, and malnutrition.<sup>7,8</sup> There is currently no standard of care for radiation induced salivary gland dysfunction; treatment is often limited to palliative therapeutics that provide only temporary relief.<sup>8,9</sup> Further, as previously mentioned, cases of OSCC are now presenting in younger individuals, indicting an imperative need to ameliorate the effects of radiation therapy on salivary gland function, as these individuals may experience symptoms for many years.<sup>4,6</sup>

Three major salivary gland pairs include the submandibular, parotid, and sublingual glands. All three gland types maintain similar structure, with a central duct branching into smaller acini that contain secretory acinar cells.<sup>10</sup> In humans, the parotid gland is the largest and is composed of serous acini that produce a watery secretion in response to parasympathetic stimulation.<sup>10</sup> The submandibular and sublingual glands contain both mucous and serous acini, with fewer mucous than serous acini in the submandibular than sublingual.<sup>10</sup> The salivary glands are particularly radiosensitive, with the parotid gland being the most radiosensitive,<sup>11</sup> yet the mechanisms of the cellular response to radiation remain unclear.<sup>8</sup> Several studies have been conducted to determine the mechanism of gland damage following radiation, focusing on acinar cell apoptosis, autophagy, proliferation, DNA damage, and others.<sup>12-20</sup> Based on the variety of research and outcomes identified, it appears that the mechanism is complex and likely involves more than one cellular process.

Compensatory proliferation in the wound healing response is a process conserved across species and tissue types and has been implicated in the cellular response to radiation. While proliferation following tissue damage is typically considered beneficial to replace apoptotic and/or necrotic cells, the proliferative response in radiation-treated salivary glands occurs concomitantly with significant reductions in salivary output.<sup>21-24</sup> In 2005, Bralic et al. suggested an increase in proliferative cells following both 7.5 and 15 Gy radiation, peaking 5-7 days following radiation.<sup>24</sup> Additionally, several animal studies have proposed models of restoration that result in significant increases in salivary flow and correlate with decreases in acinar cell proliferation. Previous work indicates that administration of insulin-like growth factor-1 (IGF-1) to mice exposed to 5 Gy radiation restores glandular function and salivary output when multiple doses are administered following exposure.<sup>13,22-23</sup> Functional restoration of the gland is associated with attenuation of the proliferative response in irradiated plus IGF-1 treated mice<sup>23</sup>, possibly

indicating that the newly dividing cells have limited functional capability and are therefore not contributing to saliva production. Similarly, 5 Gy irradiated mice treated with the Rapalogue CCI-779 have improved salivary function 30 days following radiation; parotid salivary glands from these mice also show lower levels of proliferative cells compared to irradiated controls.<sup>21</sup> Further, functional restoration via pharmacological activation of the ectodysplasin/ectodysplasin receptor (EDA/EDAR) signaling pathway restores salivary gland function in radiation-treated mice. This model correspondingly shows reductions in proliferative cells in EDAR-agonist monoclonal antibody treated irradiated mouse parotid glands.<sup>25</sup> Taken together, these data suggest that reducing the proportion of proliferative cells in the parotid salivary gland may play a role in improving functionality following radiation therapy.

Several enzymes involved in cellular metabolism also play a role in cell survival, and may regulate proliferation, cell cycle arrest, DNA repair, and apoptosis. One of the most frequently studied metabolic regulators, AMP-activated protein kinase (AMPK), modulates flux through metabolic pathways in response to low energy states within the cell.<sup>26-28</sup> AMPK is activated during low energy states during starvation or stress, and phosphorylates enzymes involved in glucose, lipid, and protein metabolism and synthesis, as well as many proteins involved in redox regulation, inflammatory processes, and cellular survival.<sup>27,29-31,33</sup> AMPK is composed of three subunits. The alpha subunit contains the catalytic domain that is primarily responsible for phosphorylation of downstream substrates.<sup>27,33</sup> The gamma subunit is composed of AMP-binding domains that allow AMPK to respond to changes in the AMP:ATP ratio. AMP binding to this subunit induces a conformational change that allows for phosphorylation and subsequent activation via liver kinase B1 (LKB1), calcium-calmodulin-dependent kinase kinase 2 (CaMKK2), or TGF $\beta$ -activated kinase 1 (TAK1).<sup>27,33</sup> AMPK can be dephosphorylated and, thus, deactivated via protein phosphatase 2A (PP2A), protein phosphatase 2C (PP2C) and Mg<sup>2+</sup>/Mn<sup>2+</sup>-dependent protein phosphatase 1E (PPM1E).<sup>27,33</sup> Active AMPK plays a role in the phosphorylation of several metabolic enzymes that result in activation of catabolic processes, including fatty acid oxidation and glycolysis; AMPK can also promote autophagy to preserve cells in energy deplete conditions.<sup>27,31-33</sup> Additionally, AMPK leads to inhibition of high-energy anabolic pathways, including fatty acid synthesis, protein synthesis, and proliferation.<sup>33</sup>

In various normal and cancerous cell lines, AMPK activation is shown to inhibit cell division via numerous mechanisms.<sup>35-38</sup> The inhibitory effect of AMPK activation on cell growth and proliferation has been primarily attributed to modulation of the tumor suppressor protein, p53, and inhibition of mammalian target of rapamycin (mTOR1) signaling.<sup>34,35</sup> Jones et al. found that activation of AMPK in vascular smooth muscle cells led to a significant increase in p53 phosphorylation (p-p53) and cell-cycle arrest.<sup>35</sup> In a study aimed to determine the role of AMPK in atherosclerosis, Hao et al. treated primary cultured human aortic muscle cells with metformin, a commonly prescribed antidiabetic drug that activates AMPK. The results show that metformin treatment increased levels of p-AMPK and p-p53, as well as inhibited proliferation of these cells.<sup>39</sup> mTOR complex 1 (mTORC1) induces activation of catabolic processes, including macromolecule synthesis, growth and cell cycle progression.<sup>40</sup> AMPK has been shown to directly inhibit mTORC1 in carcinoma cells and hepatocytes, independent of p53, leading to cell growth inhibition.<sup>41,42</sup>

Although the role of AMPK in models of obesity, diabetes, and cancer has been well characterized in the literature, the function of AMPK in saliva production remains to be fully elucidated. In 2003, Stoltoff et al. induced salivary fluid secretion via treatment with carbachol and 3'-O-(4-benzoyl)benzoyl adenosine 5'-triphosphate (BzATP); both drugs also induced AMPK phosphorylation in parotid salivary gland cells.<sup>43</sup> They then investigated carbachol-stimulated AMPK phosphorylation in parotid acinar cells further and found that inhibition of the Na-K-ATPase attenuated AMPK phosphorylation, indicating that ATP depletion due to activity of this ion channel indirectly causes AMPK activation.<sup>44</sup> Another study in rat submandibular gland cells indicated that treatment with either adiponectin, a hormone known to regulate glucose and lipid metabolism, or AICAR, a well-characterized AMPK activator, promoted salivary gland secretion. Further, pharmacological AMPK inhibition abolished the effects of adiponectin and 5-Aminoimidazole-4-carboxamide ribonucleotide (AICAR), indicating a role for AMPK in adiponectin-stimulated fluid secretion.<sup>45</sup> Additional studies in salivary gland cells indicate a different role for AMPK in fluid secretion. One such study by Xiang et al. found that AMPK activation with AICAR modulated paracellular permeability in SMG cells via phosphorylation of tight junction protein claudin-4.<sup>46</sup> Although preliminary data implicate AMPK in salivary secretion, additional research is necessary to clarify these mechanisms.

Based on preliminary evidence suggesting a role for AMPK in salivary secretion, the present study aimed to 1) assess changes in NAD<sup>+</sup> and AMP levels in parotid salivary glands five days following exposure to 5 Gy ionizing radiation (IR), 2) characterize the levels of phosphorylated AMPK and enzymes in downstream pathways five days following IR, 3) determine the effect of pharmacological activation of AMPK with AICAR on radiation-induced compensatory proliferation in parotid acinar cells and 4) evaluate the effect of AICAR or metformin treatment on chronic salivary output following radiation exposure. We hypothesize that the irradiated tissue will exhibit significantly lower AMP and NAD<sup>+</sup> levels and, concurrently, phosphorylated AMPK levels will be lower at day 5 following radiation. We also hypothesize that treatment with AICAR will attenuate the well characterized proliferative response following IR and that treatment with AICAR or metformin will improve chronic (day 30) salivary output when administered at 4, 5, and 6 days following radiation.

## Materials and Methods

Ethics Statement. All mice were housed and maintained in accordance with the University of Arizona Institutional Animal Care and Use Committee (IACUC). All protocols were approved by the IACUC.

Mice. FVB mice were purchased from Jackson Laboratories (Bar Harbor, ME) and housed in cages exposed to 12-hour light/dark cycles. Mice had *ad libitum* access to food and water. Size- and age-matched four to eight week-old mice were randomly assigned to treatment groups for all experiments. Administration of metformin or AICAR was done on days 4, 5, and 6 following IR via oral gavage (metformin, 100 mg/kg body weight) or intraperitoneal injection (AICAR, 500 mg/kg body weight).

Radiation treatment. Four to eight week-old mice were sedated with a ketamine/xylazine solution (70 mg/kg, 10 mg/ml) via intramuscular injection prior to irradiation. Mice were placed in 50 ml conical tubes and shielded with >6 mm lead blocks to ensure targeted head and neck exposure. The mice were set 80 cm from the radiation source (<sup>60</sup>Co Teletherapy Unit, Theratron-80, Atomic Energy of Canada Ltd) and received a 5 Gy radiation dose (~0.5 Gy/min).

Western Blot. Parotid glands were removed from four to eight week-old FVB mice and lysed in RIPA buffer containing 5 mM sodium orthovanadate (Fisher Scientific), 1x concentration of protease inhibitor cocktail (Sigma-Aldrich) and 100 mM phenylmethylsulfonyl fluoride (Thermo Scientific). Samples were homogenized then boiled at 100°C for ten minutes, and sonicated for ~2 minutes to ensure homogenous solutions. Samples were then centrifuged at 10,000 RPM at 4°C for 15 min. and the supernatant collected. 50 ug of protein were loaded in 10% polyacrylamide gels. Protein was transferred at 100 V for 1 hour onto 0.45 um Immobilon-P membranes (Millipore), followed by blocking for 1 hour in TBST with 5% dry nonfat milk. Blocking solution was washed from membrane with TBST for 5 min. Membranes were incubated in primary antibody overnight at 4°C (Anti-p-AMPK, Cell Signaling #2531, 1:500 in TBST with 5% BSA; anti-AMPK, Cell Signaling #2603, 1:500 in TBST with 5% BSA). Membranes were washed with TBST (3 x 5 min.), followed by incubation with secondary antibody (HRP-

conjugated, Cell Signaling #7074S, 1:10,000 in TBST) for 1 hour at room temp. Membrane was washed with TBST (3 x 5 min.) and incubated in SuperSignal West Pico Plus Chemiluminescent Substrate (Thermo Scientific) for 5 min.

RNA isolation and qRT-PCR. Parotid glands were removed from four to eight week old FVB mice 3 and 5 days after 5 Gy radiation. Tissues were incubated in RNAlater (Qiagen) for 24 hours. RNA was isolated with the RNeasy Mini Kit (Qiagen) per the manufacturer's instructions, followed by DNA digestion with the RNase-free DNase set (Qiagen). RNA was diluted to 200 µg/µl for each sample and cDNA was synthesized using the SuperScript IV First-Strand Synthesis Kit (Invitrogen) with oligo (dT) and 5 µl of diluted RNA per reaction, per the manufacturer's instructions. cDNA was diluted 1:5 and used for RT-PCR analysis. RT-PCR was performed on the iQ5 Real-Time PCR detection system (Bio-Rad), using the QuantiTect SYBR green PCR Kit (Qiagen). NAMPT primers (forward: 5'-GGCTACGTGGACGACGACAC-3'; reverse: 5'-CATCCCCTGCAGGCCTGGTCT-3') and Sirt1 primers (forward: 5'-AGAGTTGCCACCAACACCTCTT-3'; reverse: 5'-TTAGGCCAGCATTTTCTCACTGT-3') were purchased from Integrated DNA Technologies (IDT). Target genes were normalized to 15S ribosomal RNA (forward: 5'-ACTATTCTGCCCCGAGATGGTG-3', reverse: 5'-TGCTTTACGGGCTTG TAGGTG- 3') also purchased from IDT.

Histology. Salivary glands were removed at days 5, 6, or 7 following exposure to 5 Gy radiation, fixed in 10% (v/v) formalin for 24 hours and sent to IDEXX Bioresearch (Columbia, MO), where they were transferred to 70% (v/v) ethanol, embedded in paraffin and sectioned into 4 µm sections, and returned for immunofluorescent staining.

Immunofluorescent staining and manual cell counting. Slides were baked at 37°C for 20 minutes ensure tissue adherence to glass prior to staining. Slides were then rehydrated in HistoClear (2 x 5 min., National Diagnostics), 100% ethanol (EtOH, 2 x 5 min.), 95% EtOH (2 x 5 min.), 70% EtOH (2 x 5 min.), 50% EtOH (2 x 5 min.), and diH2O (2 x 5 min.). Slides were then permeabilized for 15 minutes with 0.2% Triton X-100 in PBS. Antigen

retrieval was performed by microwaving slides in 100 mM citric acid (2 x 5 min.) and allowed to cool for 20 min. Slides were washed with PBS (3 x 5 min.) and non-specific binding sites were blocked with 0.5% NEN blocking solution (Perkin Elmer) at room temperature for 1 hour. Slides were incubated at 4°C overnight in primary Ki-67 antibody (Cell Signaling, #9129S) diluted 1:400 in 1% BSA in PBS, then incubated in secondary antibody (Alexa Fluor 488, Thermo Fischer). Slides were treated with 4',6-diamidino-2-phenylindole (DAPI, 1 ug/ml) nuclear stain for 3 minutes and mounted with glass coverslips in 1 drop of ProLong Gold Antifade Mounting Reagent (Thermo Scientific). Slides were imaged with a Leica DM5500 microscope (Leica Microsystems) and an ORCA-Flash4.0 LT Digital CMOS camera (Hamamatsu Photonics K.K.). At least 5 images per mouse (4-5 mice/group) were manually counted for Ki67+ and total acinar cells and compared to untreated controls.

Saliva collection. Stimulated whole saliva collection was performed on days 3 and 30 following radiation treatment. Mice were injected intraperitoneally with carbachol (0.25 mg/kg body weight) and whole saliva was collected for 5 minutes by vacuum aspiration. Saliva was collected in pre-weighed tubes and snap frozen on dry ice. Salivary flow rates were calculated by dividing the difference in tube weight by the number of minutes to determine the amount of saliva (mg) per minute of collection. These values were then normalized to the average saliva flow rate of the untreated group on each day of collection to determine the relative change in salivary output.

Statistical analysis. Statistical analysis was performed using GraphPad Prism 6 software (GraphPad Software). Manual cell counts from immunofluorescent stained slides were analyzed by ANOVA with Tukey's multiple comparisons test. Data from qRT-PCR was normalized to loading controls (GAPDH/S15) and analyzed with a t-test comparing irradiated values to untreated. Densitometry data from Western blot was analyzed using a t-test comparing untreated to irradiated values. Saliva collection data was normalized to untreated values for each collection day and compared with a one-way ANOVA with Newman-Keuls multiple comparisons test.

## Results

### **NAD<sup>+</sup> and AMP levels are lower in parotid salivary gland tissue five days following radiation.**

Radiation exposure has been shown to affect metabolism within a whole organism or specific tissue.<sup>47-49</sup> To determine metabolic changes in salivary gland tissue following radiation, uncover potential biomarkers for radiation exposure and damage, and discover new therapeutic targets to ameliorate salivary gland dysfunction following radiation, an untargeted metabolomics analysis was performed. 4-6 week old mice were irradiated and parotid glands removed at day 5 following radiation with an equal number of untreated parotid glands. Glands were sent to Metabolon and analyzed by LC-MS for NAD<sup>+</sup> and AMP levels, among many others. We observe significantly lower NAD and AMP levels in irradiated parotid salivary glands 5 days following radiation compared to untreated controls (Fig. 1A,B). These data suggest that tissue damage following radiation may alter pathways involved in NAD<sup>+</sup> and AMP metabolism.

### **Radiation suppresses parotid salivary gland AMPK phosphorylation and expression of NAMPT and SIRT1.**

Previous research in both cancerous and normal cell lines has shown changes in AMPK activity following radiation exposure.<sup>50,51</sup> To evaluate changes in active AMPK following IR in parotid salivary glands, we collected glands from four to eight week-old mice on radiation days 3 and 5 as well as untreated, extracted protein, and performed a Western blot on these samples. Phosphorylated AMPK protein levels are significantly decreased 5 days following radiation in parotid mouse salivary glands compared to untreated controls (Fig. 2A,B). Sirtuin-1 (Sirt1) and nicotinamide phosphoribosyltransferase (NAMPT), proteins involved in the NAD salvage pathway, may be regulated by AMPK activity.<sup>33,42,52-54</sup> Sirt1 and NAMPT expression are significantly lower in mouse parotid salivary glands at day 5 following radiation (Fig. 2C), occurring at the same time point as the greatest decrease in p-AMPK levels. Therefore, radiation causes alterations in p-AMPK, as well as expression of associated pathway proteins Sirt-1 and NAMPT in parotid salivary glands.

### **AICAR treatment decreases compensatory proliferation of parotid acinar cells at D6 and D7 following radiation.**

Previous research using models of functional restoration of the salivary gland indicate a decrease in compensatory proliferation following treatment that occurs concomitantly with improved salivary output.<sup>20-23</sup> Further, AMPK activation is known to inhibit proliferation by decreasing flux through anabolic pathways that require excessive ATP, inhibition of mTOR signaling and activation of p53.<sup>34-39,41,42</sup> To determine if AMPK activation has a similar effect on proliferation in the parotid salivary gland, we treated 4-6 week old FVB mice with one dose of AICAR (500 mg/kg body weight) 5 days following radiation and collected glands 6 days following radiation for histological analysis (Fig. 3A-D). Similarly, we treated 4-6 week old FVB mice with 3 doses of AICAR (500 mg/kg body weight/injection) at days 4, 5, and 6 following radiation and collected glands for histological analysis at day 7 (Fig. 3F-J). Both AICAR dosing regimens result in a decrease in Ki67+ acinar cells in parotid salivary glands following radiation compared to irradiated-only controls (Fig. 3). These data indicate that AMPK activation following IR attenuates the proliferative response to radiation in parotid salivary glands.

### **AMPK activation with either AICAR or Metformin improves salivary output 30 days following radiation.**

Reduced proliferation in irradiated salivary glands occurs with improved salivary output in previous models of restoration.<sup>20-23</sup> AMPK activation with AICAR decreases proliferation following radiation (Fig. 4), indicating potential involvement of AMPK in the wound healing response to radiation. To determine the restorative potential of pharmacological AMPK activation, we irradiated 4-6 week old mice and treated them with known AMPK activators AICAR and metformin. Treatment with AICAR (500 mg/kg body weight/injection) at days 4, 5, and 6 following radiation significantly improves salivary output compared to irradiated controls (Fig. 4C). Treatment with metformin (100 mg/kg body weight/injection) at days 4, 5, and 6 following radiation also significantly improves salivary output following radiation (Fig. 4C). Non-irradiated mice treated with three doses of AICAR have no significant difference in salivary flow compared to untreated controls; however, non-irradiated mice treated with metformin have significantly lower salivary flow rates compared to untreated controls (Fig. 4D). Taken

together, these data implicate a role for AMPK activation in preservation of salivary gland function following radiation.

## Discussion

Chronic hyposalivation remains an incurable side effect of radiation therapy; because of this, research into novel therapeutic targets is necessary. In the present study, we found that post-radiation treatment with AICAR and metformin improved salivary output 30 days following radiation (Fig. 4B). This work provides a potential new model utilizing AMPK activation via AICAR and metformin for functional salivary gland restoration that may prove safer and more cost-effective than some proposed therapies, including gene therapy and surgical strategies.<sup>55,56</sup> Although research utilizing metformin in a salivary gland damage model has yet to be explored, metformin treatment has been widely studied in other models of epithelial wound healing. In a 2017 study, Han et al. found significantly improved cutaneous wound healing in diabetic mice treated with metformin.<sup>57</sup> Further, in an aged-mouse model of cutaneous wound healing also published in 2017, metformin, as well as known AMPK activator resveratrol, improved the speed of cutaneous wound healing.<sup>58</sup> Activation of AMPK by metformin and resveratrol likely has multiple consequences, including mTOR inhibition and subsequent inhibition of protein synthesis as well as proliferation. As previously stated, compensatory proliferation in irradiated salivary glands is associated with negative functional outcomes; inhibition of proliferation and associated anabolic processes may improve cell survival and preserve acinar cell function in irradiated salivary glands.<sup>20-23</sup>

It is important to note that administration of metformin to non-irradiated tissues significantly reduced salivary output (Fig. 5). A similar study utilizing the Rapalogue CCI-779 demonstrated similar results, with significantly lower salivary flow in non-irradiated tissues compared to untreated tissue; however, post-radiation treatment with CCI-779 improved salivary output.<sup>20</sup> Both CCI-779 and metformin inhibit mTOR activity.<sup>59-63</sup> While mTOR inhibition in irradiated, stressed tissues may promote gland healing and repair, the molecular consequence of mTOR inhibition in unstressed tissues remains to be determined. It is possible that inhibition of protein synthesis by rapalogues or metformin prevents secretion of salivary proteins, thereby reducing saliva volume in normal tissues,

whereas inhibition of protein synthesis in a damaged tissue has ulterior effects. More research into the effects of metformin on normal tissues may be necessary to determine the mechanism of changes in salivary output.

There is a significant gap in knowledge of the impact of radiation exposure on cellular metabolism in the salivary glands. We observe significantly lower levels of NAD<sup>+</sup> and AMP in parotid salivary glands five days following radiation (Fig. 1A), as well as significantly lower levels of phosphorylated AMPK at the same time point (Fig. 2). NAMPT catalyzes the rate-limiting step in the NAD-salvage pathway, thus impacting intracellular NAD<sup>+</sup> levels.<sup>64</sup> In accordance with this finding, we observe significantly lower NAMPT expression at day 5 following radiation that occurs at the same time point as reduced NAD<sup>+</sup> levels (Fig.1) and phosphorylated AMPK (Fig. 3). NAMPT expression in submandibular salivary glands has been investigated previously, and results indicated that NAMPT is downregulated in submandibular glands following IR and that increasing NAMPT expression via phenylephrine treatment improves cell survival.<sup>65</sup> AMPK has been shown to regulate expression of NAMPT in skeletal muscle cells;<sup>54</sup> however, there remains a need for future studies into the effects of AMPK activation on NAMPT expression and cell survival in irradiated parotid salivary glands.

NAD<sup>+</sup> has been long associated with cell survival and is implicated in various models of ageing.<sup>66</sup> Many studies suggest that the role of NAD<sup>+</sup> in ageing is modulated by the effects of NAD<sup>+</sup> levels on sirtuin-1 (Sirt1) activity.<sup>66</sup> In the present study, we measured Sirt1 mRNA levels at day 5 following radiation and found that they are significantly lower in irradiated vs. untreated parotid glands (Fig 3). Sirt1 is a NAD-dependent histone deacetylase involved in the DNA damage response, cellular survival, and metabolism.<sup>67-69</sup> Studies dating back to 1999 in yeast indicate a role for Sir2, the yeast ortholog of mammalian Sirt1, in longevity as well as the effects of calorie restriction.<sup>70,71</sup> Further, mammalian studies suggest that Sirt1 activity affects stress resistance in cells via deacetylation of p53, NF-KB, and FOXO family proteins.<sup>72-75</sup> Dysregulation of the DNA damage response has been identified as a driver of radiation-induced salivary gland dysfunction.<sup>76</sup> In one study, Meyer et al. found significant evidence of DNA damage in irradiated parotid salivary glands, as well as significantly lower levels of Sirt1.<sup>76</sup> Further, IGF-1 treatment rescued radiation-induced loss of Sirt-1 and resulted in fewer double-stranded DNA breaks, indicating a potential role for Sirt1 in the DNA damage response following radiation.<sup>76</sup>

Future studies on hyposalivation following targeted head and neck radiation should further elucidate the mechanism of AMPK modulation of proliferation in the parotid gland as well as the impact of AMPK on salivary output. Determination of the role of AMPK activation in salivary output will provide an avenue for clinical studies utilizing metformin or other AMPK activators that may broaden treatment options available for head and neck cancer patients undergoing radiation therapy. Development of new targets for AMPK activation may also provide an additional means to utilize these findings in the future.

In conclusion, five days following radiation, phosphorylated AMPK, NAD<sup>+</sup>, AMP, Sirt1 and NAMPT levels are suppressed compared to untreated glands. Activation of AMPK both inhibits proliferation at days 5 and 7, and improves chronic salivary flow rates at day 30 following IR, as depicted in Fig 5. This work provides a novel therapeutic target for functional gland restoration following radiotherapy that could eventually provide relief for those affected by chronic hyposalivation.

**Acknowledgements:**

We wish to thank David Williams and Michael Rice for their technical assistance. This work was supported by the NIH R01 grant #DE023534. The authors declare no potential conflicts of interest.

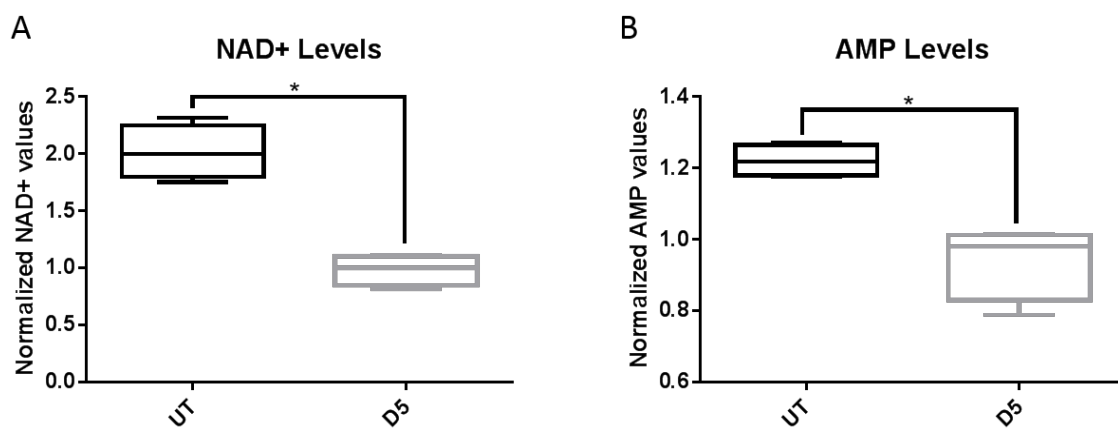


**Figure 1. NAD+ and AMP levels are lower in parotid salivary gland tissue five days following radiation.** FVB mice were either untreated (UT) or exposed to 5 Gy radiation (IR) and sacrificed at day 5 following radiation. NAD+ (A) and AMP (B) in untreated (n=4) or irradiated (n=4) parotid salivary gland tissue measured via LC-MS.

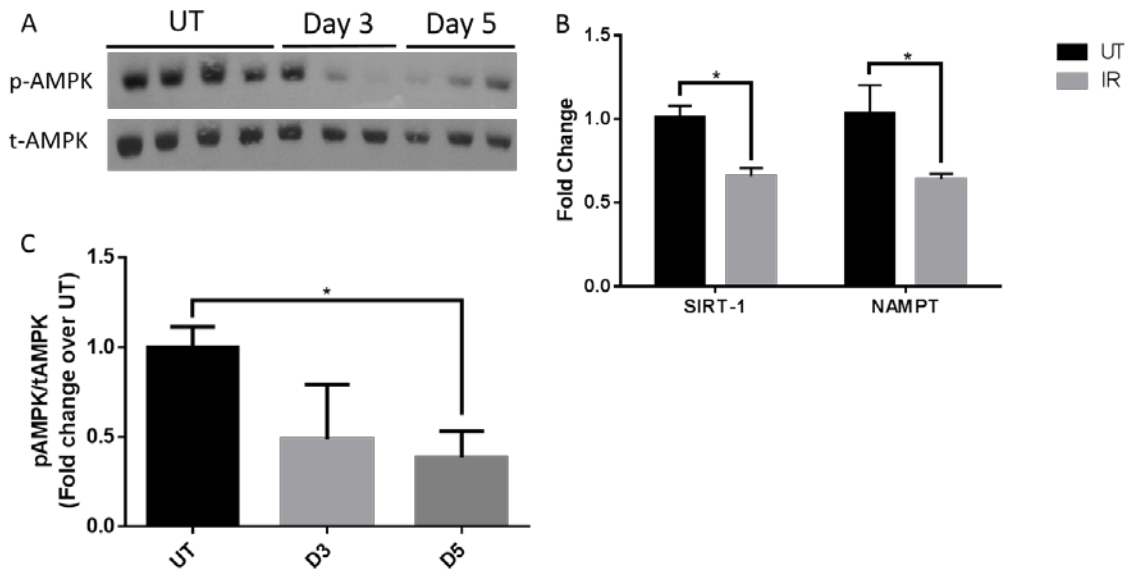


**Figure 2. Radiation suppresses parotid salivary gland AMPK phosphorylation and expression of NAMPT and SIRT1.** (A,B) Western blot analysis on samples from untreated (UT) or irradiated (IR) mice at days 3 or 5 (n=3 per group) were probed for phosphorylated and total AMPK. (C) Sirt-1 and NAMPT expression in UT or IR day 5 parotid salivary glands measured via qRT-PCR (n=4 per group).

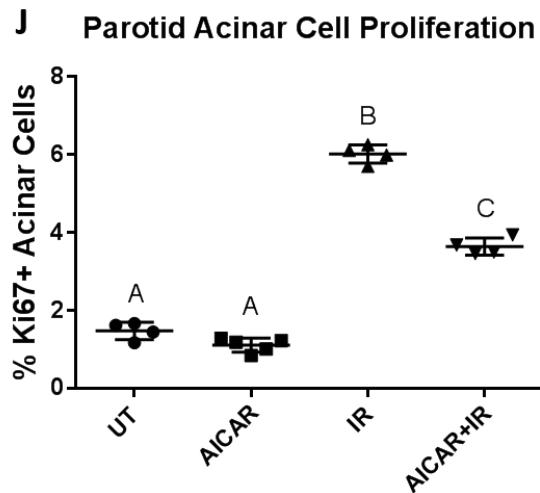
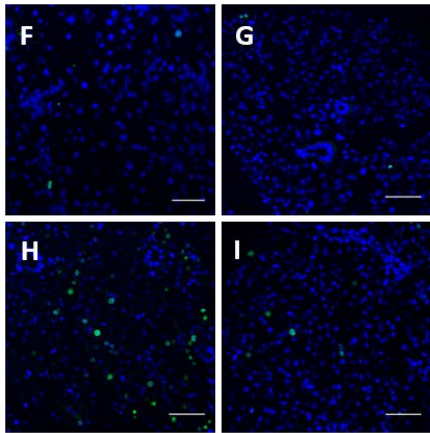
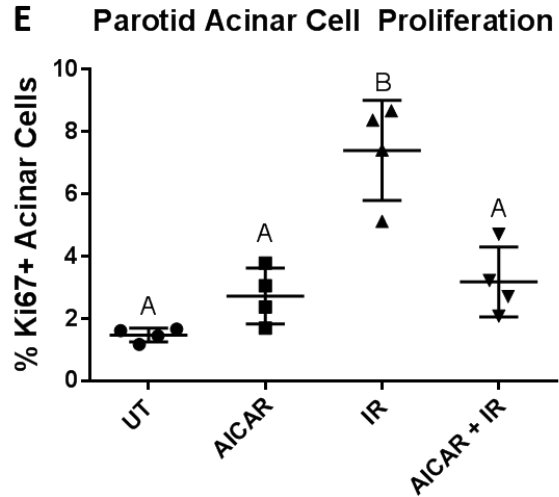
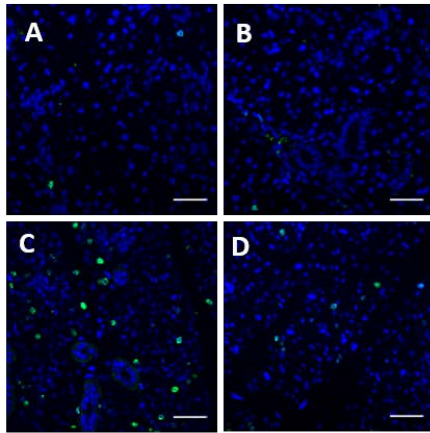


**Figure 3. AICAR treatment decreases compensatory proliferation of parotid acinar cells at D6 and D7 following radiation.** (A-D) Representative images of positive Ki67 acinar cells (green) over total nuclei stained with DAPI (blue) in (A) untreated (n=4); (B) day 6 following 5 Gy radiation (n=4), (C) treated with AICAR only (500 mg/kg) (n=4); and (D) day 6 following 5 Gy radiation and one AICAR injection (500 mg/kg) (n=5). (E) Quantification of Ki67+ nuclei as a percentage of the total number of nuclei per field of view from 5 fields of view per mouse. (F-I) Representative images of positive Ki67 acinar cells (green) over total nuclei stained with DAPI (blue) in (F) untreated (n=3); (G) day 7 following 5 Gy radiation (n=4), (H) treated with AICAR only (500 mg/kg/day, 3 days) (n=4); and (I) day 7 following 5 Gy radiation and AICAR on days 4, 5, and 6 (500 mg/kg/injection) (n=5). (E) Quantification of Ki67+ nuclei as a percentage of the total number of nuclei per field of view from 5 fields of view per mouse.

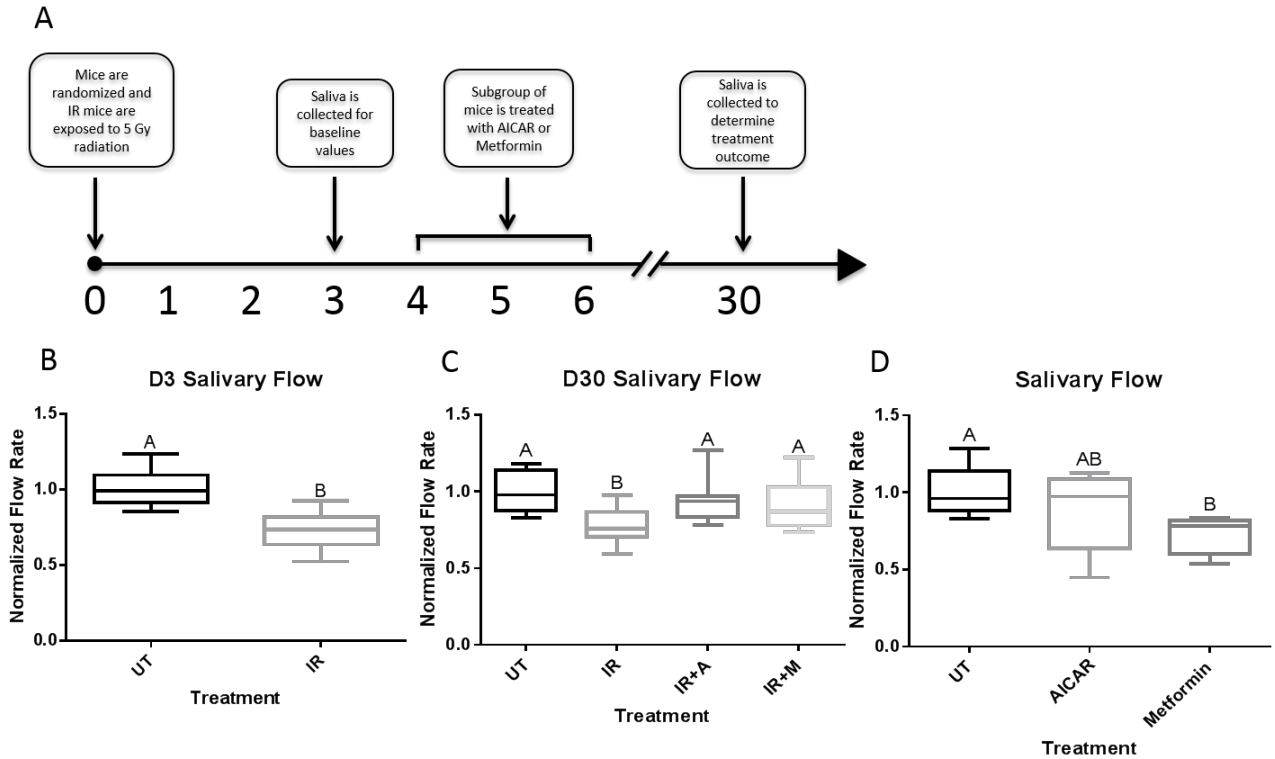


**Figure 4. AMPK activation with either AICAR or Metformin increases salivary output 30 days following radiation.** (A) Timeline of radiation and AICAR/metformin administration for salivary output experiments. (B) FVB mice were randomly assigned to receive no treatment (UT; n=18) or 5 Gy radiation (IR; n=25). Carbachol-stimulated saliva (0.25 mg/kg) was collected 3 days following radiation. (C) Irradiated mice were then randomized to receive three injections of either AICAR (500 mg/kg; n=10) or three doses of Metformin (100 mg/kg; n=8) on days 4, 5, and 6 following radiation, or no further treatment (n=17). Saliva was collected again 30 days following radiation. (D) FVB mice were randomly assigned to receive no treatment (UT, n=18), three injections of AICAR (500 mg/kg, n=8), or three doses of metformin (100 mg/kg; n=8). Carbachol-stimulated saliva (0.25 mg/kg) was collected 24 days following the final dose.

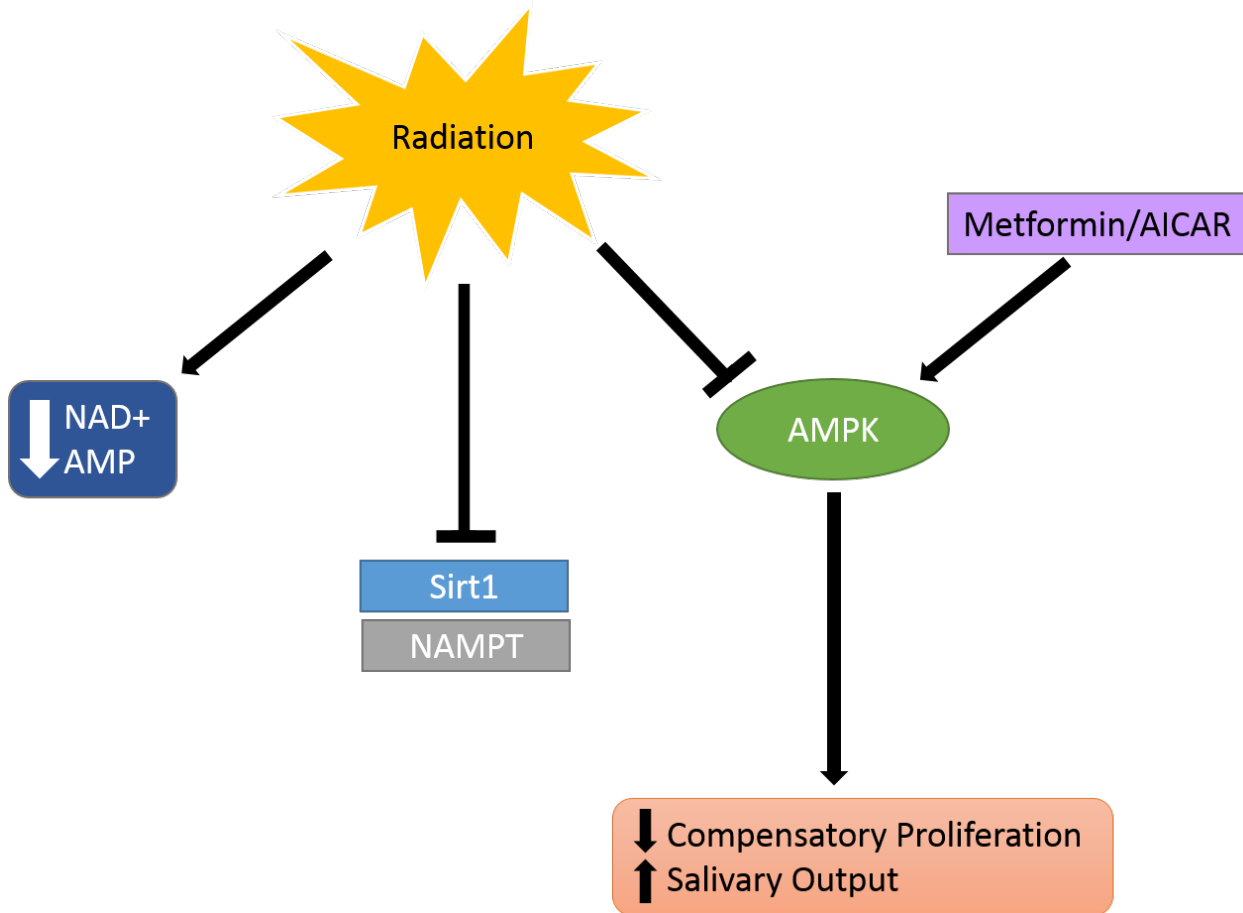


**Figure 5. Schematic representation of the role of AMP-activated protein kinase (AMPK) in radiation-induced damage to salivary glands.** Radiation decreases tissue levels of NAD<sup>+</sup> and AMP, which correlates with a decrease in phosphorylation of AMPK at day 5 post-IR. Further, NAMPT and Sirt1 expression were decreased at the same time-point. Activation of AMPK suppressed compensatory proliferation following IR and improved chronic salivary output following radiation.

## References.

1. Vigneswaran N, Williams MD. Epidemiologic trends in head and neck cancer and aids in diagnosis. *Oral Maxillofac Surg Clin North Am.* 2014;26(2):123-41.
2. Warnakulasuriya S. Global epidemiology of oral and oropharyngeal cancer. *Oral Oncology.* 2009;45(4-5):309-316.
3. Marur S, Forastiere AA. Head and Neck Squamous Cell Carcinoma: Update on Epidemiology, Diagnosis, and Treatment. *Mayo Clinic Proceedings.* 2016;91(3):386-396. doi:10.1016/j.mayocp.2015.12.017.
4. Ramqvist T, Dalianis T. Oropharyngeal cancer epidemic and human papillomavirus. *Emerg Infect Dis.* 2010;16(11):1671-7.
5. Serrano B, Brotons M, Bosch FX, Bruni L. Epidemiology and burden of HPV-related disease. *Best Practice & Research Clinical Obstetrics & Gynaecology.* 2018;47:14-26.
6. Gillison ML. Evidence for a Causal Association Between Human Papillomavirus and a Subset of Head and Neck Cancers. *Journal of the National Cancer Institute.* 2000;92(9):709-720.
7. Vissink A, Mitchell JB, Baum BJ, et al. Clinical management of salivary gland hypofunction and xerostomia in head-and-neck cancer patients: successes and barriers. *Int J Radiat Oncol Biol Phys.* 2010;78(4):983-91.
8. Grundmann O, Mitchell GC, Limesand KH. Sensitivity of salivary glands to radiation: from animal models to therapies. *J Dent Res.* 2009;88(10):894-903.
9. Chibly AM, Nguyen T, Limesand KH. Palliative Care for Salivary Gland Dysfunction Highlights the Need for Regenerative Therapies: A Review on Radiation and Salivary Gland Stem Cells. *J Palliat Care Med.* 2014;4(4):1000180.
10. Holmberg KV, Hoffman MP. Anatomy, biogenesis and regeneration of salivary glands. *Monogr Oral Sci.* 2014;24:1-13.
11. Li Y, Taylor JM, Ten Haken RK, Eisbruch A. The impact of dose on parotid salivary recovery in head and neck cancer patients treated with radiation therapy. *Int J Radiat Oncol Biol Phys.* 2006;67(3):660-9.
12. Avila JL, Grundmann O, Burd R, Limesand KH. Radiation-induced salivary gland dysfunction results from p53-dependent apoptosis. *Int J Radiat Oncol Biol Phys.* 2009;73(2):523-9.
13. Limesand KH, Said S, Anderson SM. Suppression of radiation-induced salivary gland dysfunction by IGF-1. *PLoS One.* 2009;4(3):e4663.
14. Limesand KH, Avila JL, Victory K, et al. Insulin-like growth factor-1 preserves salivary gland function after fractionated radiation. *Int J Radiat Oncol Biol Phys.* 2010;78(2):579-86.
15. Maimets M, Rocchi C, Bron R, et al. Long-Term In Vitro Expansion of Salivary Gland Stem Cells Driven by Wnt Signals. *Stem Cell Reports.* 2015;6(1):150-62.
16. Emmerson E, May AJ, Berthoin L, et al. Salivary glands regenerate after radiation injury through SOX2-mediated secretory cell replacement. *EMBO Mol Med.* 2018;10(3):e8051.
17. Aure MH, Konieczny SF, Ovitt CE. Salivary gland homeostasis is maintained through acinar cell self-duplication. *Dev Cell.* 2015;33(2):231-7.
18. Chibly AM, Querin L, Harris Z, Limesand KH. Label-retaining cells in the adult murine salivary glands possess characteristics of adult progenitor cells. *PLoS One.* 2014;9(9):e107893. Published 2014 Sep 19. doi:10.1371/journal.pone.0107893
19. Wie SM, Wellberg E, Karam SD, Reyland ME. Tyrosine Kinase Inhibitors Protect the Salivary Gland from Radiation Damage by Inhibiting Activation of Protein Kinase C- $\delta$ . *Mol Cancer Ther.* 2017;16(9):1989-1998.
20. Morgan-Bathke M, Hill GA, Harris ZI, et al. Autophagy correlates with maintenance of salivary gland function following radiation. *Sci Rep.* 2014;4:5206. Published 2014 Jun 6. doi:10.1038/srep05206
21. Morgan-Bathke M, Harris ZI, Arnett DG, et al. The Rapalogue, CCI-779, improves salivary gland function following radiation. *PLoS One.* 2014;9(12):e113183. Published 2014 Dec 1. doi:10.1371/journal.pone.0113183
22. Chibly AM, Wong WY, Pier M, et al. aPKC $\zeta$ -dependent Repression of Yap is Necessary for Functional Restoration of Irradiated Salivary Glands with IGF-1. *Sci Rep.* 2018;8(1):6347. Published 2018 Apr 20. doi:10.1038/s41598-018-24678-4

23. Grundmann O, Fillinger JL, Victory KR, Burd R, Limesand KH. Restoration of radiation therapy-induced salivary gland dysfunction in mice by post therapy IGF-1 administration. *BMC Cancer*. 2010;10:417. Published 2010 Aug 10. doi:10.1186/1471-2407-10-417
24. Bralic M, Muhvic-Urek M, Stemberga V, et al. Cell Death and Cell Proliferation in Mouse Submandibular Gland during Early Post-irradiation Phase. *Acta Medica Okayama*. 2005;59(4):153-159. doi:10.18926/AMO/31948
25. Hill G, Headon D, Harris ZI, Huttner K, Limesand KH. Pharmacological activation of the EDA/EDAR signaling pathway restores salivary gland function following radiation-induced damage. *PLoS One*. 2014;9(11):e112840. Published 2014 Nov 19. doi:10.1371/journal.pone.0112840
26. Hardie DG, Carling D, Carlson M. THE AMP-ACTIVATED/SNF1 PROTEIN KINASE SUBFAMILY: Metabolic Sensors of the Eukaryotic Cell? *Annual Review of Biochemistry*. 1998;67(1):821-855. doi:10.1146/annurev.biochem.67.1.821
27. Ke, R. , Xu, Q. , Li, C. , Luo, L. and Huang, D. (2018), Mechanisms of AMPK in the maintenance of ATP balance during energy metabolism. *Cell Biol Int*. 42: 384-392.
28. Zaha VG, Young LH. AMP-activated protein kinase regulation and biological actions in the heart. *Circ Res*. 2012;111(6):800–814. doi:10.1161/CIRCRESAHA.111.255505
29. Zhao Y, Hu X, Liu Y, et al. ROS signaling under metabolic stress: cross-talk between AMPK and AKT pathway. *Mol Cancer*. 2017;16(1):79. Published 2017 Apr 13. doi:10.1186/s12943-017-0648-1
30. O'Neill LAJ, Hardie DG. Metabolism of inflammation limited by AMPK and pseudo-starvation. *Nature*. 2013;493(7432):346-355. doi:10.1038/nature11862
31. Ha J, Guan K-L, Kim J. AMPK and autophagy in glucose/glycogen metabolism. *Molecular Aspects of Medicine*. 2015;46:46-62. doi:10.1016/j.mam.2015.08.002
32. Zhao B, Qiang L, Joseph J, Kalyanaraman B, Viollet B, He YY. Mitochondrial dysfunction activates the AMPK signaling and autophagy to promote cell survival. *Genes Dis*. 2016;3(1):82–87. doi:10.1016/j.gendis.2015.12.002
33. Jeon SM. Regulation and function of AMPK in physiology and diseases. *Exp Mol Med*. 2016;48(7):e245. Published 2016 Jul 15. doi:10.1038/emmm.2016.81
34. Imamura K, Ogura T, Kishimoto A, Kaminishi M, Esumi H. Cell Cycle Regulation via p53 Phosphorylation by a 5'-AMP Activated Protein Kinase Activator, 5-Aminoimidazole- 4-Carboxamide-1- $\beta$ -Ribofuranoside, in a Human Hepatocellular Carcinoma Cell Line. *Biochemical and Biophysical Research Communications*. 2001;287(2):562-567. doi:10.1006/bbrc.2001.5627.
35. Jones RG, Plas DR, Kubek S, et al. AMP-Activated Protein Kinase Induces a p53-Dependent Metabolic Checkpoint. *Molecular Cell*. 2005;18(3):283-293. doi:10.1016/j.molcel.2005.03.027.
36. Igata M, Motoshima H, Tsuruzoe K, Kojima K, Matsumura T, Kondo T, et al. Adenosine monophosphate-activated protein kinase suppresses vascular smooth muscle cell proliferation through the inhibition of cell cycle progression. *Circ Res*. 2005;97:837–844.
37. Zhu L, Yu X-J, Xing S, Jin F, Yang W-J. Involvement of AMP-activated Protein Kinase (AMPK) in Regulation of Cell Membrane Potential in a Gastric Cancer Cell Line. *Scientific Reports*. 2018;8(1). doi:10.1038/s41598-018-24460-6.
38. Yie Y, Zhao S, Tang Q, et al. Ursolic acid inhibited growth of hepatocellular carcinoma HepG2 cells through AMPK $\alpha$ -mediated reduction of DNA methyltransferase 1. *Molecular and Cellular Biochemistry*. 2014;402(1-2):63-74. doi:10.1007/s11010-014-2314-x.
39. Hao B, Xiao Y, Song F, et al. Metformin-induced activation of AMPK inhibits the proliferation and migration of human aortic smooth muscle cells through upregulation of p53 and IFI16. *Int J Mol Med*. 2017;41(3):1365–1376. doi:10.3892/ijmm.2017.3346
40. Laplante M, Sabatini DM. mTOR signaling in growth control and disease. *Cell*. 2012;149(2):274–293. doi:10.1016/j.cell.2012.03.017
41. Agarwal S, Bell CM, Rothbart SB, Moran RG. AMP-activated Protein Kinase (AMPK) Control of mTORC1 Is p53- and TSC2-independent in Pemetrexed-treated Carcinoma Cells. *J Biol Chem*. 2015;290(46):27473–27486. doi:10.1074/jbc.M115.665133

42. Weikel KA, Ruderman NB, Cacicedo JM. Unraveling the actions of AMP-activated protein kinase in metabolic diseases: Systemic to molecular insights. *Metabolism*. 2016;65(5):634–645. doi:10.1016/j.metabol.2016.01.005
43. Soltoff SP. Evidence That Tyrphostins AG10 and AG18 Are Mitochondrial Uncouplers That Alter Phosphorylation-dependent Cell Signaling. *Journal of Biological Chemistry*. 2003;279(12):10910–10918. doi:10.1074/jbc.m305396200.
44. Soltoff SP, Hedden L. Regulation of ERK1/2 by ouabain and Na-K-ATPase-dependent energy utilization and AMPK activation in parotid acinar cells. *Am J Physiol Cell Physiol*. 2008;295(3):C590–C599. doi:10.1152/ajpcell.00140.2008
45. Ding C, Li L, Su YC, et al. Adiponectin increases secretion of rat submandibular gland via adiponectin receptors-mediated AMPK signaling. *PLoS One*. 2013;8(5):e63878. Published 2013 May 7. doi:10.1371/journal.pone.0063878
46. Xiang R-L, Mei M, Cong X, et al. Claudin-4 is required for AMPK-modulated paracellular permeability in submandibular gland cells. *Journal of Molecular Cell Biology*. 2014;6(6):486–497. doi:10.1093/jmcb/mju048.
47. Klein S, Luu K, Sakurai Y, Miller R, Langer M, Zhang X-J. Metabolic response to radiation therapy in patients with cancer. *Metabolism*. 1996;45(6):767–773. doi:10.1016/s0026-0495(96)90144-4.
48. Golla S, Golla JP, Krausz KW, et al. Metabolomic Analysis of Mice Exposed to Gamma Radiation Reveals a Systemic Understanding of Total-Body Exposure. *Radiat Res*. 2017;187(5):612–629. doi:10.1667/RR14592.1
49. Manna SK, Krausz KW, Bonzo JA, Idle JR, Gonzalez FJ. Metabolomics reveals aging-associated attenuation of noninvasive radiation biomarkers in mice: potential role of polyamine catabolism and incoherent DNA damage-repair. *J Proteome Res*. 2013;12(5):2269–2281. doi:10.1021/pr400161k
50. Sanli T, Rashid A, Liu C, et al. Ionizing Radiation Activates AMP-Activated Kinase (AMPK): A Target for Radiosensitization of Human Cancer Cells. *International Journal of Radiation Oncology\*Biophysics\*Physics*. 2010;78(1):221–229. doi:10.1016/j.ijrobp.2010.03.005.
51. Muaddi H, Chowdhury S, Vellanki R, Zamiara P, Koritzinsky M. Contributions of AMPK and p53 dependent signaling to radiation response in the presence of metformin. *Radiotherapy and Oncology*. 2013;108(3):446–450. doi:10.1016/j.radonc.2013.06.014.
52. Cantó C, Gerhart-Hines Z, Feige JN, et al. AMPK regulates energy expenditure by modulating NAD<sup>+</sup> metabolism and SIRT1 activity. *Nature*. 2009;458(7241):1056–1060. doi:10.1038/nature07813
53. Han X, Tai H, Wang X, et al. AMPK activation protects cells from oxidative stress-induced senescence via autophagic flux restoration and intracellular NAD(+) elevation. *Aging Cell*. 2016;15(3):416–427. doi:10.1111/acer.12446
54. Brandauer J, Vienberg SG, Andersen MA, et al. AMP-activated protein kinase regulates nicotinamide phosphoribosyl transferase expression in skeletal muscle. *J Physiol*. 2013;591(20):5207–5220. doi:10.1113/jphysiol.2013.259515
55. Sood AJ, Fox NF, O'Connell BP et al (2014). Salivary gland transfer to prevent radiation-induced xerostomia: a systematic review and meta-analysis. *Oral Oncol* 50: 77–83.
56. Sasportas LS, Hosford DN, Sodini MA, et al. Cost-effectiveness landscape analysis of treatments addressing xerostomia in patients receiving head and neck radiation therapy. *Oral Surg Oral Med Oral Pathol Oral Radiol*. 2013;116(1):e37–e51. doi:10.1016/j.oooo.2013.02.017
57. Han X, Tao Y, Deng Y, Yu J, Sun Y, Jiang G. Metformin accelerates wound healing in type 2 diabetic db/db mice. *Mol Med Rep*. 2017;16(6):8691–8698. doi:10.3892/mmr.2017.7707
58. Zhao P, Sui BD, Liu N, et al. Anti-aging pharmacology in cutaneous wound healing: effects of metformin, resveratrol, and rapamycin by local application. *Aging Cell*. 2017;16(5):1083–1093. doi:10.1111/acer.12635
59. Wang Z, Liu T, Chen Y, et al. Inhibition of mammalian target of rapamycin signaling by CCI-779 (temsirolimus) induces growth inhibition and cell cycle arrest in Cashmere goat fetal fibroblasts (*Capra hircus*). *DNA Cell Biol*. 2012;31(6):1095–1099. doi:10.1089/dna.2011.1559

60. Alalem M, Ray A, Ray BK. Metformin induces degradation of mTOR protein in breast cancer cells. *Cancer Med.* ;5(11):3194–3204. doi:10.1002/cam4.896
61. Romero R, Erez O, Hüttemann M, et al. Metformin, the aspirin of the 21st century: its role in gestational diabetes mellitus, prevention of preeclampsia and cancer, and the promotion of longevity. *Am J Obstet Gynecol.* 2017;217(3):282–302. doi:10.1016/j.ajog.2017.06.003
62. Rena G, Hardie DG, Pearson ER. The mechanisms of action of metformin. *Diabetologia.* 2017;60(9):1577–1585. doi:10.1007/s00125-017-4342-z
63. Kim J, You Y-J. Regulation of organelle function by metformin. *IUBMB Life.* 2017;69(7):459-469. doi:10.1002/iub.1633.
64. Revollo JR, Grimm AA, Imai S-I. The NAD Biosynthesis Pathway Mediated by Nicotinamide Phosphoribosyltransferase Regulates Sir2 Activity in Mammalian Cells. *Journal of Biological Chemistry.* 2004;279(49):50754-50763. doi:10.1074/jbc.m408388200.
65. Bonkowski MS, Sinclair DA. Slowing ageing by design: the rise of NAD<sup>+</sup> and sirtuin-activating compounds. *Nat Rev Mol Cell Biol.* 2016;17(11):679–690. doi:10.1038/nrm.2016.93
66. Bonkowski MS, Sinclair DA. Slowing ageing by design: the rise of NAD<sup>+</sup> and sirtuin-activating compounds. *Nat Rev Mol Cell Biol.* 2016;17(11):679–690. doi:10.1038/nrm.2016.93
67. Houtkooper RH, Pirinen E, Auwerx J. Sirtuins as regulators of metabolism and healthspan. *Nat Rev Mol Cell Biol.* 2012;13(4):225–238. Published 2012 Mar 7. doi:10.1038/nrm3293
68. Haigis MC, Sinclair DA. Mammalian sirtuins: biological insights and disease relevance. *Annu Rev Pathol.* 2010;5:253–295. doi:10.1146/annurev.pathol.4.110807.092250
69. Chang HC, Guarente L. SIRT1 and other sirtuins in metabolism. *Trends Endocrinol Metab.* 2014;25(3):138–145. doi:10.1016/j.tem.2013.12.001
70. Kaeberlein M, McVey M, Guarente L. The SIR2/3/4 complex and SIR2 alone promote longevity in *Saccharomyces cerevisiae* by two different mechanisms. *Genes Dev.* 1999;13(19):2570–2580.
71. Rogina B, Helfand SL. Sir2 mediates longevity in the fly through a pathway related to calorie restriction. *Proc Natl Acad Sci U S A.* 2004;101(45):15998–16003. doi:10.1073/pnas.0404184101
72. Feige JN, Auwerx J. Transcriptional targets of sirtuins in the coordination of mammalian physiology. *Curr Opin Cell Biol.* 2008;20(3):303–309. doi:10.1016/j.ceb.2008.03.012
73. Luo J, Nikolaev AY, Imai S-I, et al. Negative Control of p53 by Sir2 $\alpha$  Promotes Cell Survival under Stress. *Cell.* 2001;107(2):137-148. doi:10.1016/s0092-8674(01)00524-4.
74. Pan W, Yu H, Huang S, Zhu P. Resveratrol Protects against TNF- $\alpha$ -Induced Injury in Human Umbilical Endothelial Cells through Promoting Sirtuin-1-Induced Repression of NF- $\kappa$ B and p38 MAPK. *PLoS One.* 2016;11(1):e0147034. Published 2016 Jan 22. doi:10.1371/journal.pone.0147034
75. Cao L, Liu C, Wang F, Wang H. SIRT1 negatively regulates amyloid-beta-induced inflammation via the NF- $\kappa$ B pathway. *Braz J Med Biol Res.* ;46(8):659–669. doi:10.1590/1414-431X20132903
76. Meyer S, Chibly AM, Burd R, Limesand KH. Insulin-Like Growth Factor-1-Mediated DNA Repair in Irradiated Salivary Glands Is Sirtuin-1 Dependent. *J Dent Res.* 2017;96(2):225–232. doi:10.1177/0022034516677529